CellPress

Immunity
Article

Segmented Filamentous Bacterium Uses Secondary and Tertiary Lymphoid Tissues to Induce Gut IgA and Specific T Helper 17 Cell Responses

Emelyne Lécuyer,[1,2] Sabine Rakotobe,[1,2,3] Hélène Lengliné-Garnier,[1,2,4] Corinne Lebreton,[1,2] Marion Picard,[1,2] Catherine Juste,[3] Rémi Fritzen,[2,5] Gérard Eberl,[6] Kathy D. McCoy,[7] Andrew J. Macpherson,[7] Claude-Agnès Reynaud,[2,5] Nadine Cerf-Bensussan,[1,2,8,*] and Valérie Gaboriau-Routhiau[1,2,3,8,*]

[1]INSERM UMR1163, Laboratory of Intestinal Immunity
[2]Université Paris Descartes-Sorbonne Paris Cité and Institut Imagine, 75015 Paris, France
[3]INRA Micalis UMR1319, 78350 Jouy-en-Josas, France
[4]AP-HP, Department of Pediatric Gastroenterology, Hôpital Necker, 75015 Paris, France
[5]INSERM UMR 1151, Institut Necker-Enfants Malades, Université Paris Descartes- Sorbonne Paris Cité, 75014 Paris, France
[6]Institut Pasteur, Lymphoid Tissue Development Unit, 75015 Paris, France
[7]Maurice Müller Laboratories, Universitätsklinik für Viszerale Chirurgie und Medizin (UVCM), University of Bern, 3008 Bern, Switzerland
[8]Co-senior authors
*Correspondence: nadine.cerf-bensussan@inserm.fr (N.C.-B.), valerie.gaboriau-routhiau@inserm.fr (V.G.-R.)
http://dx.doi.org/10.1016/j.immuni.2014.03.009

SUMMARY

Segmented filamentous bacterium (SFB) is a symbiont that drives postnatal maturation of gut adaptive immune responses. In contrast to nonpathogenic *E. coli*, SFB stimulated vigorous development of Peyer's patches germinal centers but paradoxically induced only a low frequency of specific immunoglobulin A (IgA)-secreting cells with delayed accumulation of somatic mutations. Moreover, blocking Peyer's patch development abolished IgA responses to *E. coli*, but not to SFB. Indeed, SFB stimulated the postnatal development of isolated lymphoid follicles and tertiary lymphoid tissue, which substituted for Peyer's patches as inductive sites for intestinal IgA and SFB-specific T helper 17 (Th17) cell responses. Strikingly, in mice depleted of gut organized lymphoid tissue, SFB still induced a substantial but nonspecific intestinal Th17 cell response. These results demonstrate that SFB has the remarkable capacity to induce and stimulate multiple types of intestinal lymphoid tissues that cooperate to generate potent IgA and Th17 cell responses displaying only limited target specificity.

INTRODUCTION

Recent studies have shown how mammals and the complex community of 10^{14} bacteria that inhabit their distal intestines have established mutualistic relationships that provide metabolic advantages to both partners. Yet, the considerable amount of bacteria in intimate contact with the intestinal mucosa is a major potential threat to their hosts who, in turn, have evolved a complex network of innate and adaptive immune mechanisms that cooperate to form a tightly regulated protective barrier (Hooper et al., 2012). Development of the gut immune system is initiated before birth by a genetic program that determines the formation of mesenteric lymph nodes (MLNs) and Peyer's patches (PP) (van de Pavert and Mebius, 2010). However, its full development occurs only after birth and is largely driven by the microbiota, which stimulates innate defenses, induces the formation of isolated lymphoid follicles (ILF), and activates naive T and B cells into effector T and immunoglobulin A (IgA) plasma cells that populate the gut lamina propria (LP) (reviewed in Hooper et al., 2012). Because of the seminal studies by Craig and Cebra (Craig and Cebra, 1971), PP have generally been considered a major site for the initiation of intestinal adaptive responses to the microbiota and notably IgA production. Yet, alternative sites have been suggested, including MLNs (Yamamoto et al., 2000), where bacteria can be transported by dendritic cells (Macpherson and Uhr, 2004), ILF (reviewed in Knoop and Newberry [2012]) or even LP, which was suggested to be a site for T-independent IgM to IgA switch (Macpherson et al., 2000) (Fagarasan et al., 2001) (He et al., 2007) although the later hypothesis remains controversial (Bergqvist et al., 2010) (Barone et al., 2011). Moreover, it is unclear whether initiation sites of intestinal adaptive responses might differ in response to different bacteria.

Indeed, mounting evidence indicates that the 500–1,000 bacterial species inhabiting the intestine differ in their capacity to stimulate the postnatal maturation of the gut immune system (Gaboriau-Routhiau et al., 2009) (Chung et al., 2012). Recent studies have highlighted the importance of nonculturable, host-specific species and particularly the outstanding role of segmented filamentous bacteria (SFB) (Gaboriau-Routhiau et al., 2009) (Chung et al., 2012). Thus, mouse monocolonization by this *Clostridium*-related species largely recapitulated the coordinated maturation of a large spectrum of innate and adaptive T and IgA immune responses induced by a complete mouse microbiota and markedly induced a strong T helper 17 (Th17) cell response not observed with a complex microbiota lacking SFB (Gaboriau-Routhiau et al., 2009) (Ivanov et al., 2009). A striking feature of SFB is a host-specific attachment to the ileal mucosa

and notably to the epithelium covering the PP (Chase and Erlandsen, 1976) (Tannock et al., 1984). To investigate whether adherence to PP might explain the unique immunostimulatory property of SFB and influence the intensity, specificity, and nature of adaptive immune responses induced by intestinal colonization, we have used gnotobiotic mice treated or not by a chimeric lymphotoxin β receptor-immunoglobulin (LTβR-Ig) fusion protein to inhibit the development of gut lymphoid tissue (Rennert et al., 1996). Mice were colonized with SFB and, for comparison, with the nonadherent and nonvirulent strain of *Escherichia coli* MG1655. We demonstrate that the strong immunostimulatory properties of SFB are not exclusively due to its unusual adherence to PP but also result from its remarkable ability to stimulate multiple intestinal inductive sites, which cooperate to generate both specific and nonspecific gut homeostatic IgA and Th17 cell responses. Moreover, we show that IgA responses to SFB and *E. coli* differ in their specificity and diversification profile.

RESULTS

SFB but Not *E. coli* Strongly Stimulates Germinal Centers in Peyer's Patches

We have previously observed a stronger activation of PP T cells in mice colonized by SFB (SFB mice) than by the culturable fraction of the mouse microbiota devoid of SFB (Gaboriau-Routhiau et al., 2009). Accordingly, PP of SFB mice, but not of mice colonized by *E. coli* (*E. coli* mice), displayed enlarged T cell areas and a significant upregulation of *Il17*, *Il10*, *Ifng*, and *Cd40l* mRNA expression compared with germ-free mice (see Figure S1 available online). Monocolonization by SFB was also associated with a striking expansion of PP germinal centers (GC) not observed in *E. coli* mice (Figure 1A; Figure S1A). Thus, on day 20 (d20) postcolonization, the number of PP was similar in mice colonized by SFB and *E. coli* (Table S1) but SFB mice displayed large PP with several prominent GC containing $PNA^+B220^+Ki\text{-}67^+$ B cells. These PP were comparable in size to those of conventionally raised mice and contrasted with the small PP and small clusters of PNA^+B220^+ $Ki\text{-}67^+$ B cells visible in germ-free and *E. coli* mice (Figure 1A; Figure S1A). Flow cytometry confirmed that the frequency and absolute numbers of $GL7^+B220^+$ GC B cells increased significantly in PP of SFB but not of *E. coli* mice compared to germ-free mice (Figures 1B and 1C). Reminiscent of the transitory activation of PP GC reported by Shroff et al. in mice colonized with the opportunistic bacterium *Morganella morganii* (Shroff et al., 1995), the number of $GL7^+B220^+$ GC B cells in PP of SFB mice peaked at d20 postcolonization (Figure 1C). The numbers of switched $B220^+IgA^+$ B cells and $B220^-IgA^+$ plasma cells also significantly increased in PP on d20 in SFB but not in *E. coli* mice (Figures 1D and 1E). Overall, these results showed that SFB stimulation of PP has enhanced efficiency in initiating intestinal adaptive immune responses.

SFB Induces a Strong but Much Less Specific Intestinal IgA Response than *E. coli*

To define whether the much stronger induction of PP GC by SFB than by *E. coli* influenced the intensity and specificity of IgA responses, we isolated LP cells and analyzed total and specific IgA responses by ELISpot. Such analysis was preferred to ELISA because IgA present in the intestinal lumen and in the feces can be bound to bacteria, masking the site of antigenic recognition (van der Waaij et al., 1996), and because ELISpot assays allow the enumeration of IgA secreting cells (IgA-SC). The number of IgA-SC increased progressively during monocolonization by either SFB or *E. coli* compared to germ-free mice and was not different on d60 postcolonization, between SFB and *E. coli* mice, and from that observed in conventional mice (Figure 2A). This result contrasted with the significantly lower concentration of IgA in the feces of *E. coli* than of SFB mice ($p < 0.01$) (Gaboriau-Routhiau et al., 2009; Figure S2A). Transepithelial transport of IgA might be more efficient in SFB mice because ileal polymeric immunoglobulin receptor (*Pigr*) mRNA increased in SFB but not in *E. coli* mice compared to germ-free controls (Figure S2C). Contrary to the high numbers of IgA-SC, IgM-, and IgG-SC were rare and represented less than 3% of all LP Ig-SC cells in both SFB and *E. coli* mice (data not shown).

Furthermore, by using ELISpot, we observed that a fraction of LP IgA-SC reacted against the colonizing bacterium but not against irrelevant bacterial lysates (Figure 2B). Unexpectedly, the frequency of such specific LP IgA-SC was however much lower in SFB mice (3%–5%) than in *E. coli* mice (over 30%), and these figures remained stable from d20 to d60 postcolonization (Figure 2C). Together, these data showed that IgA responses to SFB and *E. coli*, although displaying comparable kinetics, differed in their specificity.

IgA Plasma Cells Induced by SFB Show Slow Accumulation of Somatic Mutations and Large Clonal Diversity

To examine further how the distinct stimulation of PP GC by SFB and *E. coli* influenced the characteristics of the IgA responses, we analyzed IgA plasma cells isolated from the LP for somatic mutation of their immunoglobulin (Ig) genes at d20, d40, and d60 after colonization, with IgA-SC from germ-free mice as controls. Because the complete sequence of the V_H locus from the C3H/HeN strain is not available, we opted to monitor mutations within the J_H4 intronic sequences flanking rearranged V_HDJ_H genes. This strategy, performed at the DNA level, allows the concurrent precise determination of mutations on a single reference sequence and the enumeration of B cell clones through their V-D-J junction. As previously reported (Lindner et al., 2012), mutations were rare in cells derived from germ-free mice. They increased in both SFB and *E. coli* mice, but with very distinct kinetics (Figures 3A and 3B). In *E. coli* mice, mutations increased markedly up to d40 and declined thereafter. In contrast, mutations were almost absent at d20 in SFB mice, suggesting that a first wave of unmutated plasma cells displaced those generated in germ-free conditions. Mutations slowly accumulated over the time period studied, reaching levels similar to the one observed in *E. coli* mice by d60. At that time, large clonal expansions were only observed in *E. coli* mice (Figure 3C). Altogether, the slow accumulation of mutations within Ig genes and the large clonal diversity of IgA plasma cells observed in SFB mice paradoxically suggest that the strong stimulation of PP GC by SFB fostered nonspecific rather than specific IgA responses. Finally, this antibody

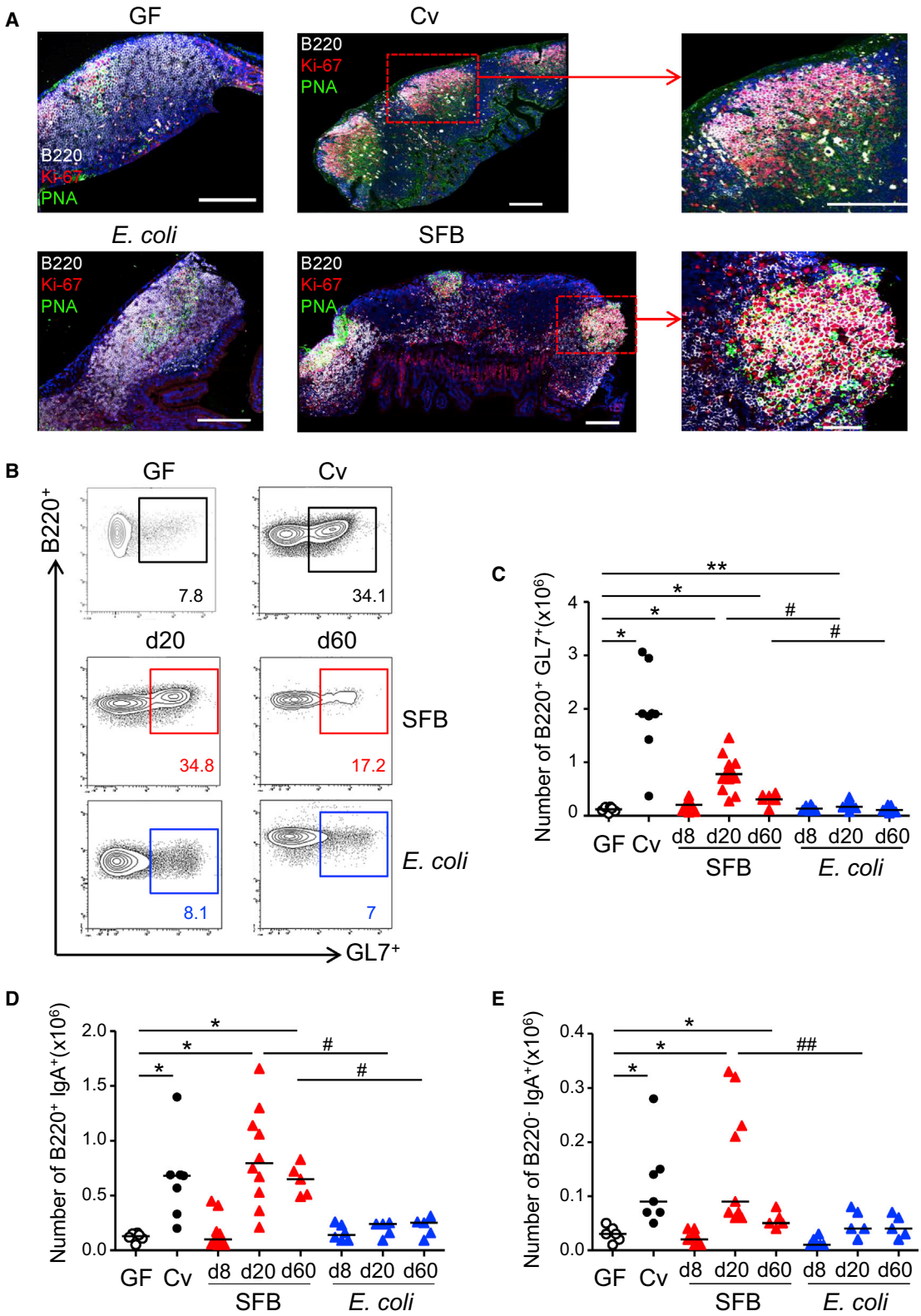

Figure 1. SFB But not *E. coli* Strongly Stimulates Germinal Centers in Peyer's Patches

(A) Staining of B220$^+$ (white), Ki-67$^+$ (red), and PNA$^+$ (peanut agglutinin; green) cells in Peyer's patches (PP) from the terminal ileum of germ-free (GF) C3H/HeN mice colonized at 8–9 weeks of age with SFB or *E. coli* MG1655 for 20 days, or of age-matched GF or conventional (Cv) C3H/HeN mice. Scale bars represent 150 μm. See also Figure S1 and Table S1.

(legend continued on next page)

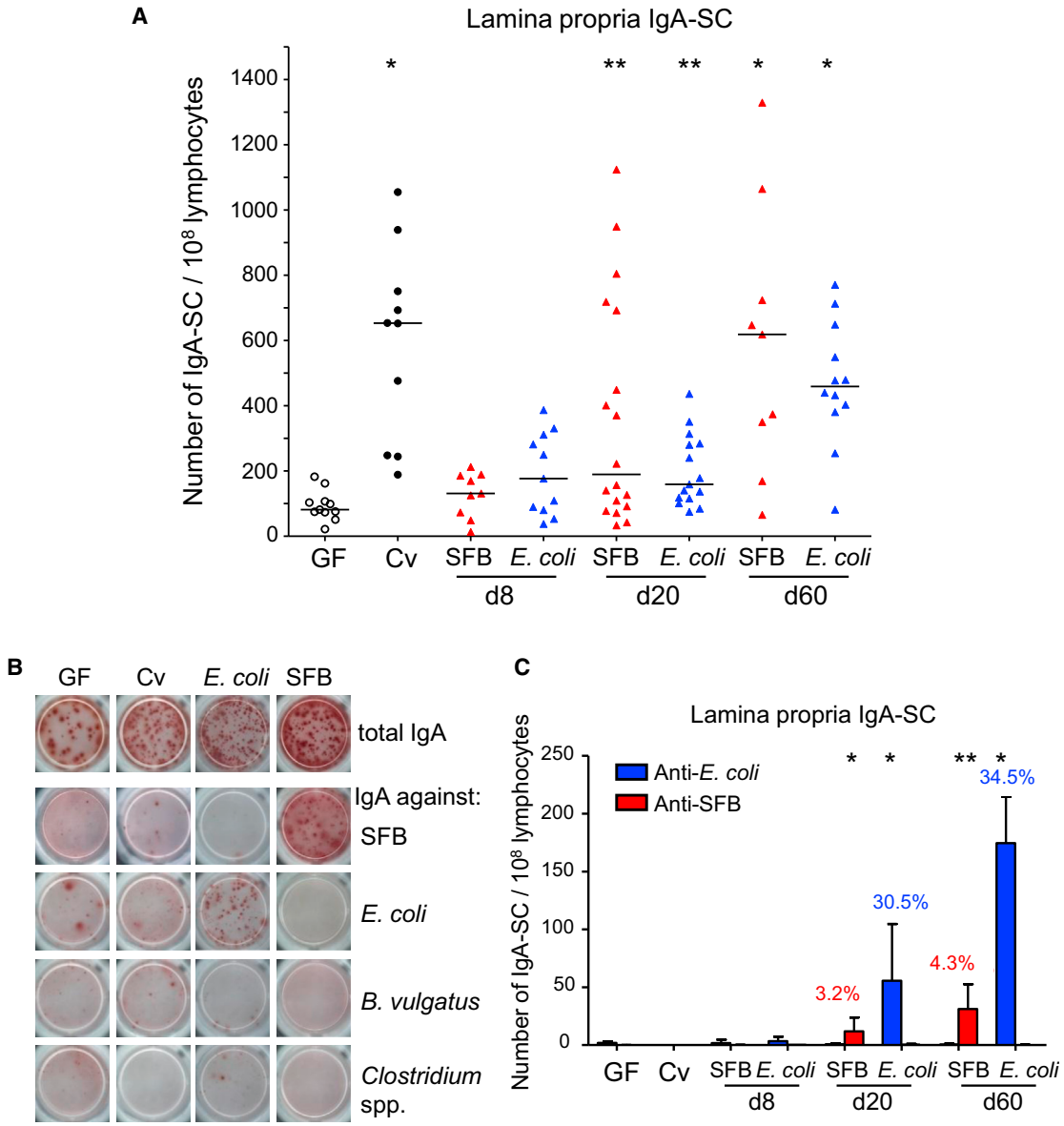

Figure 2. SFB Induces Strong But Much Less Specific Intestinal IgA Response than *E. coli*

(A) Numbers of total IgA-SC assessed by ELISpot in the lamina propria (LP) of germ-free (GF), conventional (Cv), and SFB- or *E. coli*-monocolonized mice at indicated time points after colonization. Data represent individual values and medians.

(B and C) Reactivity of IgA-SC from LP against SFB lysate, *E. coli* lysate, or irrelevant bacterial lysates from *Bacteroides vulgatus* and *Clostridium* strains, assessed by ELISpot. (B) Representative ELISpot. (C) Numbers of specific IgA-SC. Error bars represent means ± SD (n = 9–18 mice/group). Numbers indicate mean percentages of specific reactivity against SFB and *E. coli*. Lack of reactivity against *B. vulgatus* and *Clostridium* lysates is shown in (B).

**p < 0.05, *p < 0.01 compared to GF mice, by a nonparametric Mann-Whitney test. See also Figures S2A–S2C.

response of low specificity does not alter adherence of SFB to the mucosa because the amounts of SFB detected by qRT-PCR in the ileal mucosa were comparable in *Igh-J*$^{-/-}$ and wild-type (WT) C57BL/6 mice monocolonized by SFB (Figure S3).

SFB but Not *E. coli* Induces Intestinal IgA Responses in the Absence of PP and Cryptopatch-Derived ILF

The data above highlighted important differences in the characteristics of the IgA responses induced by SFB and *E. coli*. To define whether such differences might reflect distinct

(B–E) Flow cytometry analysis of B cells among CD45$^+$ cells in PP of 11-week-old GF and Cv mice and in mice colonized by SFB or *E. coli* for the indicated time. Frequency (B, representative dot-plots) and absolute numbers (C) of B220$^+$GL7$^+$ lymphocytes. Absolute numbers of B220$^+$IgA$^+$ (D) and B220$^-$IgA$^+$ (E) lymphocytes. Data in C, D, and E represent individual values and medians.

**p < 0.05, *p < 0.01 compared to GF mice and, ##p < 0.05, #p < 0.01 compared to SFB-colonized mice, by a nonparametric Mann-Whitney test.

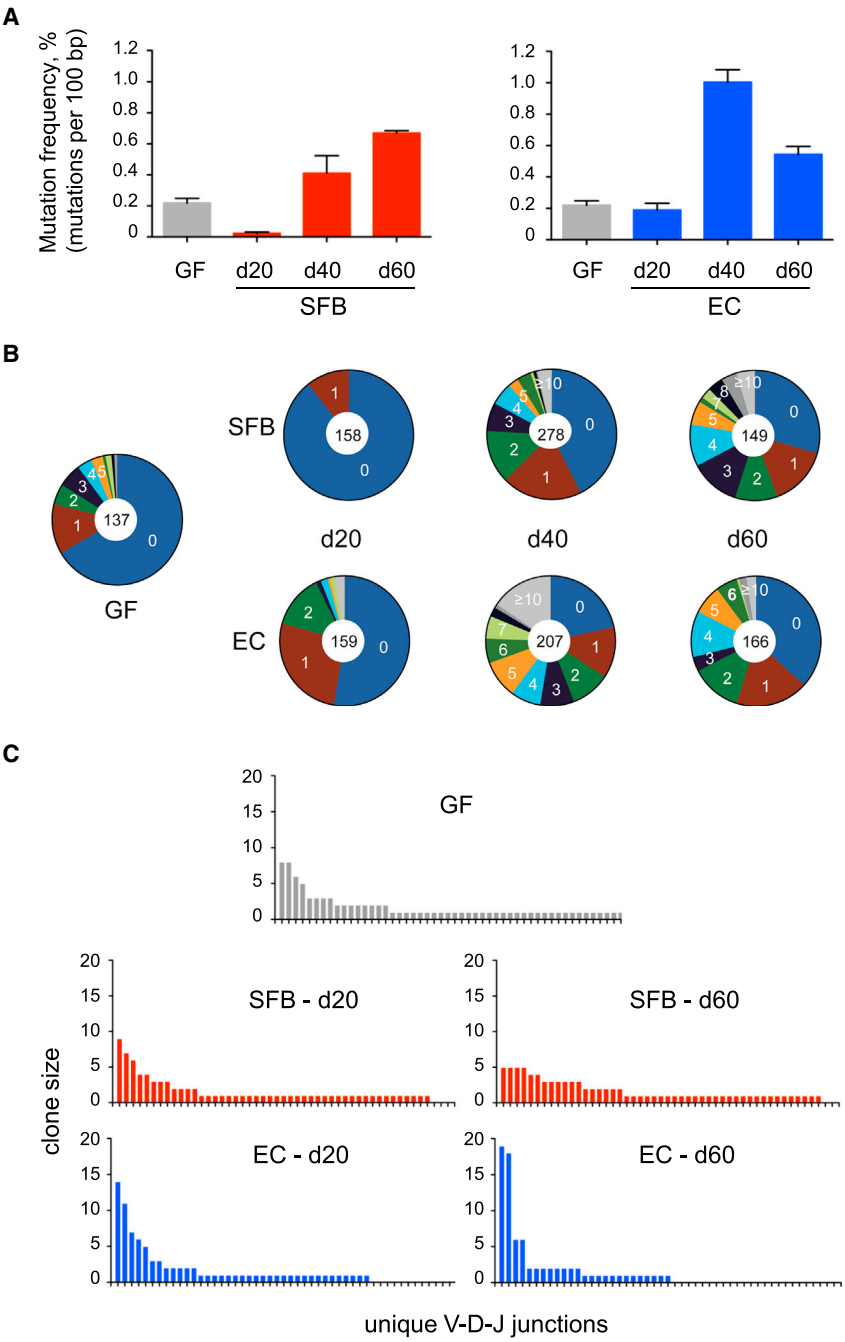

Figure 3. Lamina Propria Plasma Cells from SFB Mice Display a Slow Accumulation of Mutations with Time, in the Absence of Major Clonal Expansions

(A) Mutation frequency (number of mutations per hundred base pairs) in rearranged J_H4 intronic sequences from germ-free (GF) and from SFB and *E. coli* (EC) mice at different time points after colonization. Two mice were analyzed for each point. Error bars represent means ± SD.

(B) Accumulation of mutations within individual J_H4 intronic sequences. The relative proportion of sequences harboring a given number of mutations is represented (with mutation numbers), and the total number of sequences analyzed is indicated in the center of the pie chart.

(C) Clonal expansions within LP plasma cells from individual mice. Each B cell clone (corresponding to a unique V-D-J junction) is represented by one bar along the abscissa line, with the total number of sequences sharing the same junction plotted as ordinate for five representative mice (for which similar number of sequences, between 78 and 89, were determined). Clones identified by a single sequence are overrepresented in GF and SFB mice compared to *E. coli* mice.

See also Figure S3.

dependence on PP, we examined IgA responses in PP-deficient mice. Pregnant germ-free mice were treated with LTβR-Ig fusion protein to inhibit the development of PP (Rennert et al., 1996) (Figure 4A). The PP-deficient (PP^-) offsprings were then monocolonized at 8 weeks of age by either SFB or *E. coli*, and LP IgA responses were assessed by ELISpot on d8 and d20 postcolonization. No macroscopically visible PP could be detected in LTβR-Ig-treated mice, confirming the efficacy of the antenatal treatment (Table S1; Figure S4B). The number of IgA-SC was markedly decreased in PP^- mice monocolonized by SFB compared with untreated mice, demonstrating a substantial contribution of PP to SFB-induced plasma cell response (Figure 4B). Yet, a small but significant increase in the number of LP IgA-SC was observed on d20 compared to d8 postcolonization ($p < 0.05$) (Figure 4B). As in untreated mice, very few Ig-SC were specific for SFB (data not shown) and there was no increase in IgM- or IgG-SC (Figure 4B). In marked contrast, IgA-SC did not increase in the LP of PP^- mice monocolonized by *E. coli* (Figure 4B). Thus, SFB, but not *E. coli*, could stimulate an intestinal IgA response in the absence of PP. A suggested alternative site of initiation of IgA responses are cryptopatch-derived ILF (Tsuji et al., 2008). A group of mice was therefore treated with LTβR-Ig fusion protein not only antenatally to prevent the development of PP but also during the first 3 weeks of life to inhibit the postnatal development of cryptopatches and of the derived ILF (Bouskra et al., 2008) (Figure 4A; Table S1). Strikingly, a significant increase in LP IgA-SC was observed between d8 and d20 in SFB ($p < 0.01$) but not in *E. coli* mice lacking both PP and cryptopatch-derived ILF (PI^- mice) (Figure 4B). In agreement with these findings, concentrations of fecal IgA were significantly higher on d20 in the feces of PI^- SFB mice than of germ-free mice ($p < 0.04$) (Figure S2A). Together, these data show that SFB, but not *E. coli*, could initiate an IgA response outside of PP and cryptopatch-derived ILF.

SFB Can Induce IgA Responses via the De Novo Induction of Tertiary Lymphoid Tissue

It was suggested that the IgM-to-IgA switch can take place in the intestinal LP independently of cognate T cell help and GC formation following interactions of a proliferation-inducing ligand (APRIL) with the transmembrane activator and CALM interactor (TACI) on B cells (He et al., 2007; He et al., 2010). Consistent with this hypothesis, *April* mRNA was increased in the ileum of SFB mice with or without PP, as compared to germ-free mice (Figure 4C). Yet, the LP of conventional mice and of SFB mice contained more $B220^+GL7^+$ GC B cells than germ-free or *E. coli* mice (Figures 4D and 4E), suggesting that SFB stimulated the development of ILF-containing GC outside PP. In agreement, immunohistochemical staining showed ILF containing PNA^+ $B220^+Ki\text{-}67^+$ GC B cells and numerous $CD4^+$ T cells in the small intestine of SFB and conventional mice, whereas germ-free and *E. coli* mice only displayed small ILF containing $B220^+$ cells negative for PNA and Ki-67 (Figure 5; Figures S4 and S5; Table S1; data not shown). ILF containing clusters of PNA^+B220^+ $Ki\text{-}67^+$ GC B cells and $CD4^+$ T cells were also visible in intestinal rolls of SFB mice lacking PP (Figure 5). Strikingly, substantial numbers of GC B cells were detected in the LP of LTβR-Ig-treated SFB mice lacking both PP and cryptopatch-derived ILF (Figures 4D and 4E). Moreover, ILF containing PNA^+B220^+ $Ki\text{-}67^+$ GC B cells and $CD4^+$ T cells were detected in the small intestine (Figure 5). Together, these results indicate the de novo induction of tertiary lymphoid tissue by SFB and contrast with the lack of induction of ILF in *E. coli* mice lacking PP and cryptopatch-derived ILF (Figure S5; Table S1). Of note, RORγt-deficient mice, which lack PP and cryptopatch-derived ILF, can nevertheless develop tertiary lymphoid tissue in response to microbiota and inflammatory stimuli (Lochner et al., 2011b). Such an inflammatory stimulus might be provided by SFB. Thus, a robust induction of inducible nitric oxide synthase 2 (*Nos2* or *Inos*) transcripts was observed in the ileum of only SFB but not of *E. coli* mice, whether mice were treated with LTβR-Ig or not (Figure 4C). To demonstrate the role of tertiary lymphoid tissue in the IgA response of SFB mice lacking PP and ILF, we also treated germ-free mice injected with LTβR-Ig before birth and in the neonatal period two days before and during the 3 weeks of colonization with SFB (PI^-Lt group) (Figure 4A). On d20 postcolonization, B cell follicles were undetectable in tissue sections of SFB-PI^-Lt mice (Figure S4), LP contained neither $B220^+GL7^+$ GC B cells (Figures 4D and 4E) nor IgA-SC (Figure 4B), and fecal IgA were hardly detectable (Figure S2A). Moreover, *April* transcripts were no longer detected in LP (Figure 4C). Overall, these results indicated that tertiary lymphoid tissue induced by SFB were able and required to initiate IgA response to SFB in mice lacking PP and ILF.

MLN and Spleen Are Not Inductive Sites for IgA Responses to SFB or *E. coli*

Whether MLN might substitute for organized gut lymphoid tissue in initiating IgA responses to the microbiota is debated. It is also unclear whether the microbiota induces IgA responses in the spleen. Antibody responses to SFB and *E. coli* were therefore analyzed in MLN and spleen of mice with or without LTβR-Ig treatment. Compared to germ-free mice, *E. coli* mice displayed a modest but significant increase in the number of IgA-SC in MLN and spleen on d20 postcolonization ($p < 0.01$), which was abolished in mice lacking PP (Figures 6A–6C). A more robust expansion of IgA-SC was observed in the MLN and spleen of SFB mice (30- and 10-fold compared to germ-free mice on d20 postcolonization, respectively) (Figures 6A–6C). In SFB mice lacking PP or PP and ILF, induction of IgA-SC was significantly reduced in the spleen ($p < 0.01$) but not in MLN (Figure 6). The induction of IgA-SC was however abolished in both MLN and spleen in SFB mice lacking all gut lymphoid tissue after long-term treatment with LTβR-Ig (Figure 6). In the MLN of the latter mice, the lack of IgA-SC contrasted with a significant increase in IgG-SC ($p < 0.01$) (Figure 6B), indicating that the capacity of MLN to mount a B cell response to SFB was not impaired by LTβR-Ig treatment and that IgG, but not IgA, were generated in MLN. In line with these results, SFB, but not *E. coli*, mice displayed a significant increase in serum IgA compared with germ-free mice ($p < 0.01$ for NT SFB mice, and $p < 0.04$ for PP^- and PI^- SFB mice), and this response was abolished in SFB mice lacking all gut lymphoid tissue (Figure S2B). Overall, these data demonstrate that MLN are not a site of initiation of the IgA responses to either *E. coli* or SFB but suggest that IgA-SC induced in PP, ILF, or tertiary lymphoid tissue by the microbiota, and in particular by SFB, migrate from the gut to the MLN and spleen.

SFB Initiates Gut Th17 Responses in and Outside Gut Organized Lymphoid Tissue

One hallmark of the intestinal response induced by SFB is a strong expansion of Th17 cells (Gaboriau-Routhiau et al., 2009). Accordingly, anti-CD3 + anti-CD28-stimulated LP lymphocytes (LPL) from SFB mice secreted 1,200-fold more interleukin-17 (IL-17) than LPL from germ-free mice (Figure 7A), and intracellular staining indicated that SFB colonization induced the appearance of IL-17-secreting $CD4^+$ T cells both in LPL and PP (Figures S6A and S6B). We therefore examined the reactivity of LP Th17 cells against SFB and the role of gut organized lymphoid tissue in their stimulation. LPL from SFB mice produced large amounts of IL-17 when stimulated by an SFB lysate but not by lysates from irrelevant Gram-positive or Gram-negative bacteria (Figure 7A), indicating that the intestinal Th17 cell response was at least partially specific for SFB. Moreover, IL-17 was induced by the SFB lysate in LPL from conventional mice, which contained SFB in their microbiota, but not in LPL from germ-free or *E. coli* mice (Figure 7A; data not shown). Notably, the Th17 cell response to SFB lysate was restricted to LPL and was detected neither in MLN nor in spleen cells of SFB mice, even if the latter cells produced significantly more IL-17 in response to anti-CD3 + anti-CD28 stimulation than those from germ-free mice ($p < 0.01$) (Figures S6C and S6D; data not shown). In contrast to the strong induction of IL-17-producing cells in SFB mice, the amount of IL-17 secreted by LPL from *E. coli* mice in response to anti-CD3 + anti-CD28 stimulation was approximately 1% of that produced by LPL from SFB mice (Figure 7A). This result was consistent with the paucity of $IL\text{-}17^+$ $CD4^+$ T cells in both the LP and PP of *E. coli* mice (Figures S6A and S6B). LPL from *E. coli* mice also did not produce IL-17 in response to *E. coli* lysate (Figure 7A). Yet, this lysate could stimulate the secretion of IL-17 by LPL from conventional mice

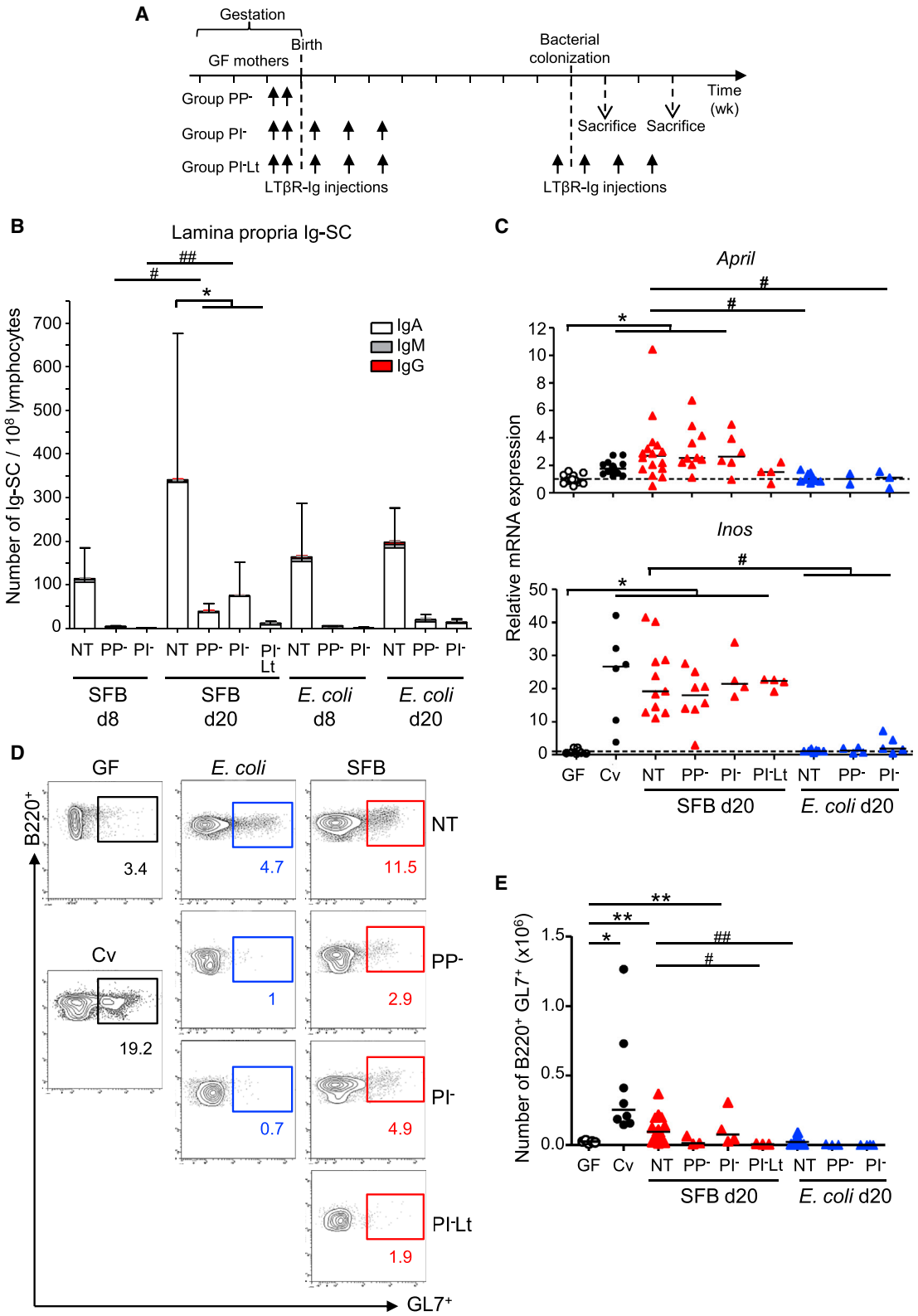

Figure 4. Peyer's Patches and Cryptopatch-Derived ILF Are Partially Dispensable for IgA Response to SFB

(A) Diagram depicting LTβR-Ig treatment. C3H/HeN germ-free (GF) pregnant mice were treated with LTβR-Ig fusion protein (arrows) on d16 and d18 of gestation to prevent the development of PP in their offspring (group PP$^-$). Some pups were also treated in the neonatal period (group PI$^-$) or for long-term period

(legend continued on next page)

(Figure 7A; p = 0.012 compared to irrelevant bacterial lysates), suggesting that colonization by a complex microbiota containing SFB might facilitate the development of specific Th17 cell responses against other bacteria.

Strikingly, PP and cryptopatch-derived ILF were fully dispensable for SFB-induced Th17 cell response. Thus, the secretion of IL-17 by LPL in response to CD3 and CD28 antibodies or to SFB lysate was unchanged in PP^{-} and PI^{-} mice, compared with control SFB mice (Figure 7B). IL-17 production by anti-CD3 + anti-CD28-stimulated LPL was also modestly reduced in PI^{-}Lt SFB mice, which are deprived of PP and ILF and cannot develop de novo tertiary lymphoid tissue during colonization. However, in PI^{-}Lt SFB mice, LPL were unable to produce IL-17 in response to the SFB lysate (Figure 7B). Interestingly, in MLN cells of SFB mice, CD3 and CD28 antibodies (but not SFB lysate, data not shown) induced a small secretion of IL-17, which persisted in the absence of PP and cryptopatch-derived ILF, but not of tertiary lymphoid tissue (Figure S6D). Therefore, SFB induces an SFB-specific IL-17 response that requires organized lymphoid tissue including tertiary lymphoid tissues, but also a sizeable nonspecific Th17 cell response, which can arise independently of organized lymphoid tissue. In keeping with this result, the weak secretion of IL-17 induced by CD3 and CD28 antibodies in LPL of *E. coli* mice was not modified by LTβR-Ig treatment (Figure S6E).

DISCUSSION

To date, how SFB orchestrate the coordinated postnatal maturation of innate and adaptive intestinal immune responses remains poorly understood. Here we demonstrate that SFB can stimulate multiple intestinal inductive sites, which cooperate to generate some specific but mostly non-specific gut homeostatic IgA and Th17 cell responses.

Consistent with previous reports (Talham et al., 1999; Gaboriau-Routhiau et al., 2009; Ivanov et al., 2009), monocolonization by SFB induced a large expansion of LP IgA plasma cells and IL-17-secreting T cells, as well as a strong innate response attested by the upregulation of a spectrum of ileal transcripts. In contrast, *E. coli* MG1655 induced almost exclusively a conspicuous expansion of LP IgA-SC, a result reminiscent of that observed in mice colonized with the culturable fraction of the gut microbiota, which displayed a large bacterial diversity in their feces but lacked SFB (Gaboriau-Routhiau et al., 2009). We therefore used *E. coli* MG1655 as a surrogate bacterium to mimic the effect of the bulk of culturable commensal bacteria and to facilitate the comparison with SFB. One first plausible hypothesis to explain the outstanding immunostimulatory role of SFB was its adherence to PP, a major site of induction of gut adaptive immune responses. Accordingly, PP of SFB mice displayed strongly stimulated T cells and an explosive development of GC not observed in mice colonized by *E. coli*. Yet, unexpectedly, we observed that PP were indispensable for the intestinal IgA response to *E. coli* MG1655 but not to SFB, because IgA-SC were markedly reduced but still induced in SFB mice lacking PP. Moreover and strikingly, the intestinal Th17 cell response was not modified. An intestinal IgA response was still observed in SFB mice lacking not only PP but also cryptopatch-derived ILF after postnatal treatment with LTβR-Ig, raising the possibility that IgM to IgA switch might take place in LP (He et al., 2007). Yet, we observed that the LP of SFB mice lacking both PP and cryptopatch-derived ILF displayed GC-containing gut lymphoid tissue and that LTβR-Ig treatment during SFB colonization simultaneously prevented the development of all gut-associated lymphoid structures and abolished the intestinal IgA response. This treatment also abolished the small induction of IgA-SC observed in the MLN and spleen of control SFB mice. We therefore conclude that gut-associated lymphoid tissue is indispensable to induce IgA responses to two prototype members of the microbiota and notably to SFB. Whether this conclusion can be extended to the IgA response induced by a complex microbiota needs to be established as the onset of IgA responses outside gut organized lymphoid tissue remains a debated issue (Macpherson et al., 2000; Fagarasan et al., 2001; He et al., 2007). In SFB mice, treated or not with LTβR-Ig, the development of ILF containing GC and $CD4^{+}$ T cells suggests that T cell-dependent IgA responses might take place outside PP. Nevertheless, the presence of GC does not exclude a T cell-independent mechanism. Notably, both T-dependent and T-independent IgA induction can take place in PP (Bergqvist et al., 2010). Further studies will be needed to delineate the respective contribution of the two mechanisms in the generation of IgA in SFB and *E. coli* mice. Our results also stress the importance of checking for the induction of tertiary lymphoid tissue when analyzing the initiation sites of adaptive intestinal responses. The de novo development of gut tertiary lymphoid tissue was recently described during colitis induced by dextran sulfate sodium (DSS) in RORγt-deficient mice, which lack PP and cryptopatch-derived ILF (Lochner et al., 2011b). In DSS-treated $Rorc^{-/-}$ mice, which cannot produce IL-17, the development of tertiary lymphoid tissue was dependent on the microbiota and was associated with a strong inflammatory response dominated by the production of interferon-γ and tumor necrosis factor alpha, and a prominent serum IgG response. Here we provide the first demonstration that in RORγt-proficient mice,

(group PI^{-}Lt) to prevent the development of PP and ILF or of all gut organized lymphoid tissues, respectively. Mice were colonized at 8 weeks of age with SFB or *E. coli* and were sacrificed on d8 or on d20 postcolonization. Untreated mice (group NT) colonized at adult age were used as controls. See also Table S1.

(B) Numbers of total IgA-, IgG-, and IgM-SC in the LP of mice, assessed by ELISpot. Error bars represent means ± SD for each isotype (n = 4–12 mice/group). Significant differences in the numbers of IgA-SC between LTβR-Ig-treated and NT SFB mice on d20 postcolonization (*p < 0.01), and between d8 and d20 postcolonization in LTβR-Ig-treated mice (#p < 0.05 and ##p < 0.01) were assessed by a nonparametric Mann-Whitney test. See also Figure S2A.

(C) mRNA expression of *April* and *Inos* analyzed by qRT-PCR in ileal biopsies on d20 postcolonization, and in germ-free (GF) or conventional (Cv) age-matched mice. mRNA expression is relative to GF mice (defined as 1; dotted line).

(D and E) Frequency (D; representative dot-plots) and absolute numbers (E) of $B220^{+}GL7^{+}$ B lymphocytes isolated from LP of mice GF, Cv, or monocolonized with SFB or *E. coli* for 20 days and assessed by flow cytometry.

Data in (C) and (E) represent individual values and medians. **p < 0.04, *p < 0.01 compared to GF mice and, #p < 0.01, ##p < 0.03 compared to NT SFB mice, by a nonparametric Mann-Whitney test. Data for LTβR-Ig-treated mice are pooled from three independent experiments.

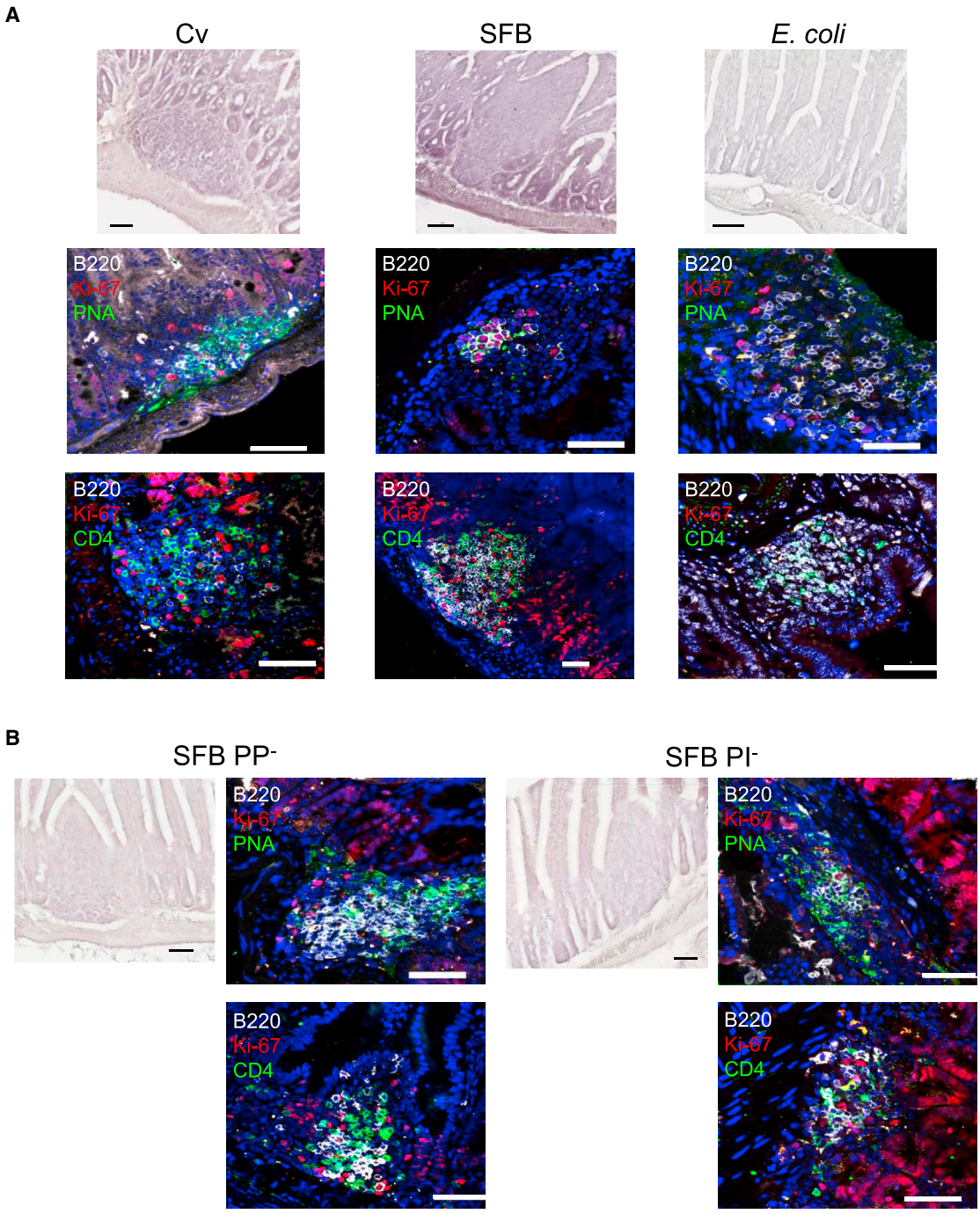

Figure 5. SFB Induces De Novo Tertiary Lymphoid Follicles Containing Germinal Centers

Intestinal rolls from conventional (Cv) mice and from mice colonized with SFB or *E. coli* for 20 days were stained with hematoxylin and eosin, or with B220 (white), Ki-67 (red), and either PNA (peanut agglutinin; green) or CD4 (green) antibodies.

Isolated lymphoid follicles from mice nontreated (A) or treated with LTβR-Ig (B) to eliminate PP (PP^{-}) or PP and cryptopatch-derived ILF (PI^{-}) are shown. Scale bars represent 50 μm. See also Figures S4, S5 and Table S1.

gut tertiary lymphoid tissue can be an inductive site for IgA response and can also entirely substitute for PP and cryptopatch-derived ILF to initiate a Th17 response displaying reactivity against SFB. Moreover, we show that LPL of mice lacking gut-associated lymphoid tissue could not produce IL-17 when stimulated by SFB, but remained capable to produce large amounts of IL-17 in response to a polyclonal stimulation by anti-CD3 and anti-CD28 antibodies. As discussed below, these data suggest that Th17 cells are generated along two different pathways in the small intestine.

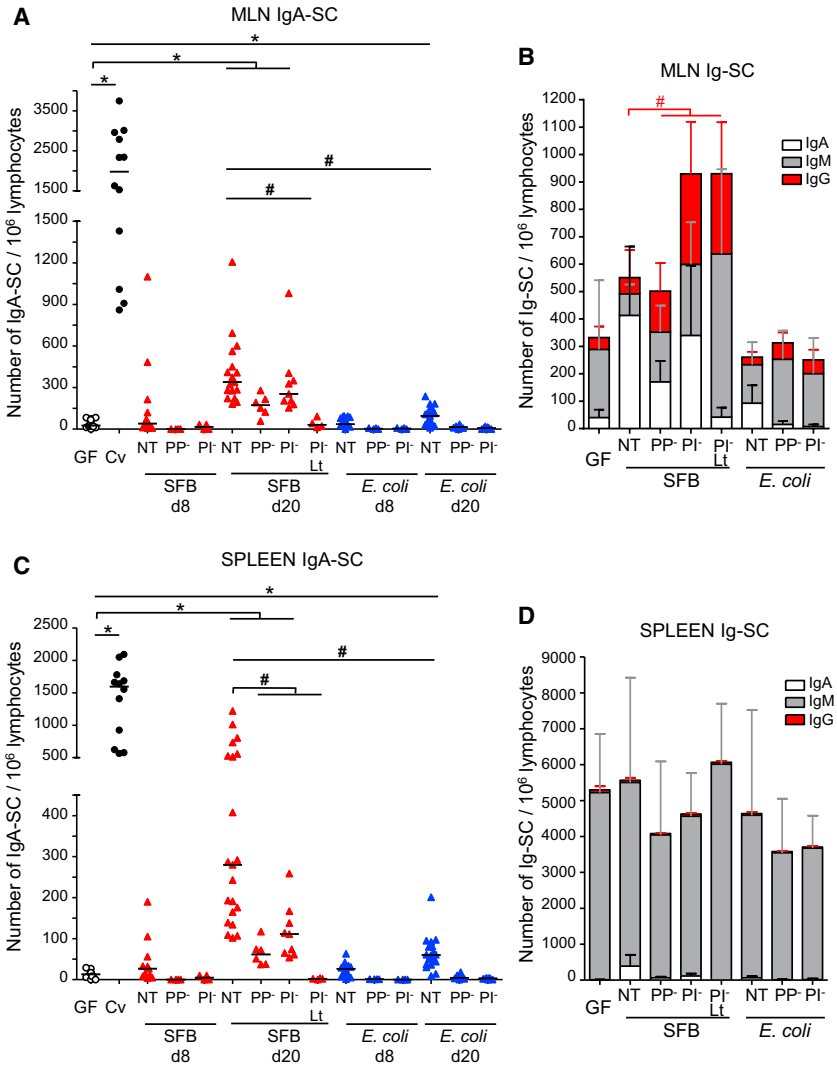

Figure 6. Organized Gut Lymphoid Tissues Are Necessary for Initiating IgA Responses to SFB and *E. coli* in MLN and Spleen

(A–C) Numbers of total IgA-SC assessed by ELISpot in MLN (A) and spleen (C) of C3H/HeN mice germ-free (GF), conventional (Cv), and colonized with SFB or *E. coli* for 8 and 20 days, and treated or not with LTβR-Ig as in Figure 4. Data represent individual values and medians. *$p < 0.01$ compared to GF mice and, #$p < 0.01$ compared to NT SFB mice on d20, by a nonparametric Mann-Whitney test. See also Figures S2A and S2B. (B–D) Numbers of total IgA-, IgG-, and IgM-SC in MLN (B) and spleen (D) of mice defined as in (A), on d20 postcolonization. Error bars represent means ± SD for each Ig subclass. #$p < 0.01$ for IgG-SC between LTβR-Ig-treated and control NT SFB mice.

Our choice to work in mice monocolonized by SFB and *E. coli* was largely dictated by the possibility to compare the reactivity of the adaptive responses against these two prototypic bacteria. Indeed, the specificity of the intestinal T and B cell responses induced by the microbiota remains a disputed question and it is not known whether it might vary between bacteria. The coexistence of three types of intestinal IgA have been suggested: "natural" IgA, which are produced in germ-free mice and display negligible reactivity against the microbiota; "primitive" IgA, which are produced rapidly and independently of T cell help, display no or rare somatic mutations, and show low avidity and cross-reactivity to some microbial or autoantigens; and finally "classical" T cell-dependent IgA, which display somatic mutations and substantial avidity and specificity against microbial antigens, notably those that are pathogen-derived (reviewed in Slack et al. [2012]). A recent analysis of clones derived from human LP IgA plasma cells has further suggested that the vast majority of these cells failed to react with any tested auto or microbial antigens (Benckert et al., 2011). The considerable diversity of the microbiota precludes, however, to precisely quantify the specificity of the homeostatic IgA response in humans and in conventional mice and to define whether it may vary against distinct members of the microbiota. Our results in monocolonized mice highlight a striking inverse relationship between the capacity of SFB and *E. coli* to stimulate GC expansion and the frequency of IgA-SC specificity to the colonizing bacterium. Thus, PP GC did not significantly expand in *E. coli* mice compared with germ-free mice but LP plasma cells contained a high frequency of specific IgA-SC and accumulated somatic mutations within their Ig genes. Conversely, the exuberant and rapid development of GC-containing PP and ILF in SFB mice contrasted with the very low frequency of IgA-SC reactive with SFB, already noted in earlier studies (Talham et al., 1999), and with the very slow accumulation of mutations. The small number of somatic mutations observed in LP CD138$^+$ cells isolated from germ-free mice was notably undetectable in SFB mice at d20 postcolonization, indicating that SFB stimulated a first wave of mostly unmutated intestinal IgA plasma cells. The number of somatic mutations then increased progressively until d60 postcolonization, similar to what was recently described in mice colonized by a complex microbiota (Lindner et al., 2012). The strong stimulation of GC, notably during the early phase of the colonization by SFB, might perhaps promote the nonspecific activation and IgM to IgA switch of a large number of B cells, which rapidly leave the gut-associated lymphoid tissue and migrate into LP. The progressive accumulation of somatic mutations might then result, as suggested, from the recirculation of microbiota-induced memory B cells through PP GC (Lindner et al., 2012). Yet, and surprisingly, the frequency of SFB-specific IgA-SC did not increase with time and remained largely less than that of *E. coli*-specific IgA-SC. Moreover, no significant reactivity of LP IgA-SC from SFB mice (or *E. coli* mice) could be demonstrated against irrelevant bacterial lysates. Therefore, our data plead against the view that a large fraction of the antibody response induced by the microbiota might be cross-reactive but show that SFB, in

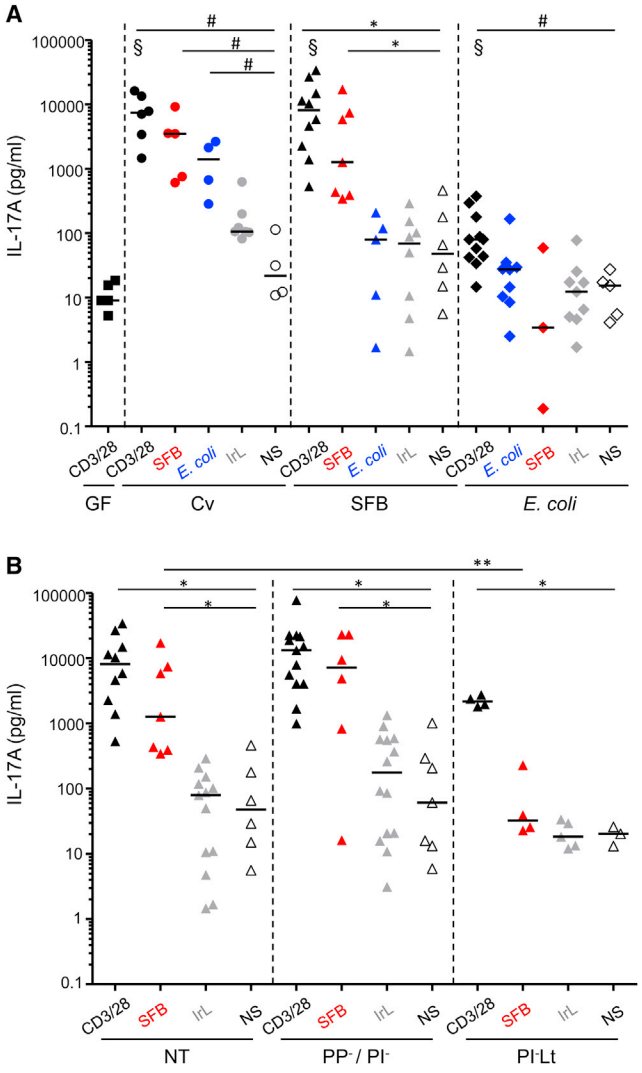

Figure 7. SFB Initiates a Specific IL-17 Response in Gut Organized Lymphoid Tissue and a Nonspecific Intestinal Th17 Response Outside Organized Lymphoid Tissue

(A) Bio-Plex quantification of IL-17A secretion in 72 hr-culture supernatants of LP lymphocytes isolated from the small intestine of mice germ-free (GF), conventional (Cv), or colonized with SFB or *E. coli* for 20 days, and stimulated by CD3 and CD28 antibodies (black symbols), SFB lysate (red symbols), *E. coli* lysate (blue symbols), irrelevant *B. vulgatus* or *Clostridium* lysates (IrL; gray symbols), or left nonstimulated (NS; open symbols).

(B) Quantification of IL-17A secretion as in (A), by LP cells from mice treated or not with LTβR-Ig, as indicated in Figure 4, and monocolonized with SFB for 20 days. IL-17 secretion in response to irrelevant lysates from *E. coli*, *B. vulgatus*, or *Clostridium* are shown together (IrL; gray symbols).

All data represent individual values and medians. §$p < 0.01$ compared to GF mice, #$p < 0.02$ and *$p < 0.01$ compared to nonstimulated cells and, **$p < 0.02$ compared to SFB-specific responses from nontreated (NT) SFB mice, by a nonparametric Mann-Whitney test. See also Figure S6.

contrast to *E. coli*, can induce a large repertoire of IgA-SC without restricted target specificity. Previous observations in mice lacking activation-induced cytidine deaminase have suggested that IgA is necessary to restrain SFB colonization (Suzuki et al., 2004). However, we did not observe an increase in SFB in the ileal mucosa of *Igh-J*$^{-/-}$ mice, lacking antibodies of all isotypes.

Data concerning the reactivity of intestinal T cells against the microbiota remain scarce. Compelling recent evidence showed that a substantial number of Foxp3^{+} CD4^{+} T cells present in the colon of conventionally housed mice harbor a T cell receptor (TCR) enabling recognition of microbiota-derived antigens (Lathrop et al., 2011) (Cebula et al., 2013). In contrast, analysis of *Rag2*$^{-/-}$ mice expressing a transgenic TCR unable to react with microbial antigens suggested that gut Th17 cell responses can develop independently of TCR recognition (Lochner et al., 2011a). This possibility is supported by our results showing that LP cells from SFB mice deprived of gut lymphoid tissue can produce large amounts of IL-17 when stimulated by CD3 and CD28 antibodies, but not by SFB. However, we also show that SFB can use constitutive or inducible gut organized lymphoid tissue and stimulate the priming of Th17 cells targeting specifically SFB. That this response depends on TCR recognition remains, however, to be proven. Notably, this SFB-specific response was exclusively observed in the LPL of SFB mice but not in MLN and spleen, supporting previous suggestions that specific T cell responses to the microbiota are compartmentalized in the intestine in immunoproficient mice (Slack et al., 2009).

In conclusion, our results highlight the outstanding capacity of SFB to orchestrate the postnatal development of organized gut lymphoid tissue and to use multiple intestinal sites to induce conspicuous IgA and Th17 cell responses displaying only limited target specificity. SFB thus differed strikingly from a nonpathogenic and nonadherent strain of *E. coli*, which induced a much more specific IgA response strictly dependent on PP. We suggest that SFB adherence to the ileal mucosa induces a strong innate response, which stimulates the development of gut lymphoid tissue and promotes the intestinal Th17 cell response. Future work will be necessary to identify the pathway(s), as well as the putative epithelial receptor for SFB, and confirm their contribution to the outstanding effect of SFB on gut immune responses.

EXPERIMENTAL PROCEDURES

Mice

Conventional and germ-free C3H/HeN and C57BL/6 mice, either WT or *Igh-J*$^{-/-}$, were bred at the INRA facilities in Jouy-en-Josas. Germ-free and gnotobiotic mice were maintained in plastic isolators and fed ad libitum on a commercial diet (R03-40; UAR) sterilized by gamma irradiation (40 kGy). To prevent the development of gut lymphoid tissues, we intravenously (i.v.) injected germ-free pregnant C3H/HeN mice with 150 μg LTβR-Ig (kind gift from J. Browning, BiogenIdec) on gestational days 16 and 18 as described (Rennert et al., 1996) (Group PP^{-}). Some germ-free C3H/HeN pups born from LTβR-Ig-treated mothers were further intraperitoneally (i.p.) injected with 10 μg LTβR-Ig once a week during the first 3 weeks of life (Group PI^{-}). Finally, some of the latter mice were also i.p. injected with 100 μg LTβR-Ig 2 days before and weekly during colonization by SFB until day 20 postcolonization (Group PI^{-}Lt) (Figure 4A).

For colonization, 8- to 9-week-old female germ-free mice were gavaged twice at a 24 hr-interval with 0.5 ml of fresh anaerobic cultures of *E. coli* MG1655 or of fecal homogenate from SFB monoassociated mice (Gaboriau-Routhiau et al., 2009). Colonization by *E. coli* was monitored by bacterial counts after culture on nonselective brain heart infusion agar plates (Difco). For SFB monitoring, DNA was extracted from frozen ileal biopsies and 16S rRNA was amplified by qRT-PCR by using specific primer pairs for SFB or total

bacteria on an ABI Prism 7300 Sequence Detection System (Life Technologies) as described (Gaboriau-Routhiau et al., 2009).

Gnotobiotic mice were sacrificed on d8, d20, and d60 postcolonization in parallel with age-matched conventional and germ-free controls. Mice were handled in accordance with European guidelines, and experiments were approved by the local ethical committee.

Quantitation of Mouse Gene Expression by Real-Time PCR

Ileal tissue and whole PPs were lysed in RNAplus by using a ribolyser FastPrep® (both MP Biomedicals). Cell suspensions were lysed in RLTplus (QIAGEN). RNA was extracted using RNeasy kit (QIAGEN). Reverse transcription of total RNA and qRT-PCR was performed on an ABI Prism 7300 Sequence Detection System using either TaqMan gene-expression assays with TaqMan Universal PCR master mix or mouse specific primers with SYBR-Green PCR master mix for *Inos* and *April* (sequences available on demand) (all reagents from Life Technologies). cDNA samples were assayed in duplicates and gene expression levels for each sample were normalized relative to TATA-box Binding Protein or to Transferrin Receptor using ΔCt calculation. MRNA expression in gnotobiotic mice is relative to expression in germ-free mice.

Bacterial Lysates

Lysates of *E. coli* MG1655, *Bacteroides vulgatus*, and nonidentified *Clostridium* strain were prepared from overnight cultures in 500 mL luria broth medium (Difco) in anaerobic conditions. SFB lysates were derived from pooled ileal and cecal contents of SFB-monoassociated *Igh-J*$^{-/-}$ mice diluted in PBS 0.01M-0.03% sodium deoxycholate (Sigma), and enriched in bacteria by centrifugation through a Nycodenz gradient (Eurobio & AbCys; 60% in PBS-0.03% sodium deoxycholate) for 90 min at 18,000 g, at 4°C. SFB were collected at the PBS/Nycodenz interface and diluted in PBS, and bacteria were pelleted for 7 min at 4,000 g. Pellet was resuspended in PBS and spun for 3 min at 300 g to eliminate debris. Supernatant was collected and spun for 7 min at 4,000 g. Bacterial pellet was suspended in 1 mL PBS and lysed by freezing at −20°C and by 6 pulses of sonication on a sonicator cell disrupter (Thermofisher Scientific). Protein concentration was determined by a Bradford assay (BioRad).

Analysis of Cytokine Production

Single cell suspensions were prepared from spleen, MLN, PP, and LP as described (Gaboriau-Routhiau et al., 2009) and resuspended in DMEM-Glutamax added with 8% fetal calf serum (FCS; PAA), 1 mM HEPES, 0.02 mM Folic acid, 0.67 mM L-Arginine and 0.27 mM L-Asparagine (all from Sigma) at 1.10^6 cells/mL. After culture for 72 hr in 96-well plates (BD Biosciences) coated overnight with anti-CD3 and anti-CD28 (5 μg/mL; BD Biosciences) or with 10 μg/mL of bacterial lysates, supernatants were harvested and cytokines measured using BioPlex assay (BioRad) according to manufacturer's instructions.

Flow Cytometry and Cell Sorting

Single cell suspensions were labeled for 20 min at 4°C with a cocktail of the following antibodies: FITC-anti-GL7 (clone GL7), APC-H7-anti-CD19 (clone 1D3), Alexa Fluor-anti-B220 (clone RA3-6B/2), biotinylated anti-CD138 (clone 231.2) (BD Biosciences), eFluor-450-anti-CD45 (clone 30-F11), PECy7-anti-CD3 (clone 145-2C11), PE-anti-CD43, PE-anti-IgA, PECy7-anti-IgM (Southern Biotec). Biotinylated antibody was revealed by a 15 min incubation with PE-Cy5-streptavidin (BD Biosciences). Labeled cells were analyzed with a CANTO II apparatus and Diva software or sorted with a FACS-ARIA (BD Biosciences).

Quantification of Immunoglobulins and Immunoglobulin-Secreting Cells

Quantification of total IgA in fecal samples by ELISA was performed as described (Gaboriau-Routhiau et al., 2009). Ig-SCs were assessed with enzyme-linked immunospot (ELISpot) assay as described (Dogan et al., 2009), by using multiscreen HTS 96-well plates (Millipore) coated overnight at 4°C with 50 μL/well of goat anti-mouse Ig (H$^+$L) (Southern Biotechnology; 10 μg/mL PBS) or of bacterial sonicate (40 μg/mL) to determine respectively total and bacterium-specific Ig-SCs. Nonspecific sites were blocked with 5% FCS for 3 hr at 37°C, and successive 4-fold dilutions of PP, LP, MLN and spleen lymphocytes (1.25 × 10^6 cells in the first well) were added and incubated overnight at 37°C and 5% CO_2. Ig-SC were revealed at room temperature by a 1.30 hr-incubation with HRP-conjugated anti-mouse IgA (Sigma), IgM, or IgG (Southern Biotechnology) (1 μg/mL in PBS-1% FCS; 100 μL/well), and 15 min incubation with 3-amino-9-ethylcarbazole (0.3 mg/mL in 0.2M sodium acetate buffer containing 30% H_2O_2; 150 μL/well; all from Sigma). Ig-SCs were analyzed with a stereomicroscope (AID EliSpot Reader System) and AID EliSpot 5.0 software (Autoimmun Diagnostika GMBH).

Analysis of Mutations in the J_H4 Intronic Sequence of the Igh Locus

The J_H4 intronic sequence flanking rearranged V_H gene segments was amplified by PCR from DNA of sorted CD45$^+$CD3$^-$CD138$^+$CD43$^+$ LP plasma cells. Three PCR were done for each sample with 10,000 freeze-dried sorted cells. The PCR primers used are a mixture of five FR3 primers amplifying most V_H gene families and a primer downstream of J_H4 (Delbos et al., 2005), with a denaturation step of 2 min at 98°C and 40 cycles of 15 s at 98°C, 30 s at 64°C and 30 s at 72°C, with Phusion® DNA polymerase (New England Biolabs). PCR products were cloned with the Zero Blunt cloning kit (Invitrogen) and sequences were determined with an ABI Prism 3130xl Genetic Analyzer using J_H4 primer. Mutations were identified within 440 base pairs of the J_H4 intron and analyzed with the help of CodonCodeAligner software.

Histological and Immunohistochemical Analysis of Gut Lymphoid Tissue

Swiss rolls of small intestine or PP-containing terminal ileum biopsies were fixed overnight in 4% paraformaldehyde and 30% sucrose (Sigma), embedded in Tissue Tek OCT compound (Sakura Finetek) and frozen in liquid nitrogen. Tissue sections (8 μm thick) were stained with hematoxylin and eosin, scanned with a NanoZoomer 2.0 (Hamamatsu) and analyzed with NDP.view software. Alternatively, sections were stained with rat monoclonal anti-mouse CD45R-Alexa Fluor 647 (B220) (BD PharMingen), with rabbit anti-mouse/rat Ki-67-eFluor 615 (eBioscience), and with either hamster monoclonal biotinylated PNA antibody (BD Biosciences) or rat anti-mouse biotinylated CD4 (BD PharMingen), and streptavidine-FITC (BD PharMingen). Slides were examined under a confocal microscope TCS SP5 (Leica) at 40× magnification and, for PP, mosaic merge pictures were realized with LAS-AF software (Leica). All images were analyzed with ImageJ software (National Institutes of Health).

Statistical Analysis

Statistical analysis was performed with GraphPad Prism software and the nonparametric Mann-Whitney tests. Differences were considered significant for $p < 0.05$.

SUPPLEMENTAL INFORMATION

Supplemental Information includes six figures and one table and can be found with this article online at http://dx.doi.org/10.1016/j.immuni.2014.03.009.

ACKNOWLEDGMENTS

The authors are supported by INSERM, Université Paris Descartes, INRA, and by grants from Agence Nationale pour la Recherche (ANR 2010 BLAN1317), Tornado FP7 EU grant 222720, and Fondation Princesse Grace. N.C.-B. is recipient of ERC-2013-AdG 339407-IMMUNOBIOTA. The laboratory and Institut Imagine are supported respectively by the programmes "Investissement d'Avenir" ANR-10-IAHU-01 and ANR-10-LABX-62-01. E.L. has been supported by the Marie Curie network Cross-Talk (PITN-GA-2008-215553) and by Fondation pour la Recherche Médicale. Authors thank J. Browning for providing LTβR-Ig reagent; O. Pellé, J. Mégret, and N. Montcuquet for cell-sorting experiments; M. Duriez, I. Quétier, and F. Pagès from the Immunomonitoring Plateform (Hôpital Européen Georges Pompidou) for scanning experiments and the Structure Fédérative de Recherche-Necker for providing access to the Imaging Plateform.

Received: July 11, 2013
Accepted: January 29, 2014
Published: April 17, 2014

REFERENCES

Barone, F., Vossenkamper, A., Boursier, L., Su, W., Watson, A., John, S., Dunn-Walters, D.K., Fields, P., Wijetilleka, S., Edgeworth, J.D., and Spencer, J. (2011). IgA-producing plasma cells originate from germinal centers that are induced by B-cell receptor engagement in humans. Gastroenterology *140*, 947–956.

Benckert, J., Schmolka, N., Kreschel, C., Zoller, M.J., Sturm, A., Wiedenmann, B., and Wardemann, H. (2011). The majority of intestinal IgA+ and IgG+ plasmablasts in the human gut are antigen-specific. J. Clin. Invest. *121*, 1946–1955.

Bergqvist, P., Stensson, A., Lycke, N.Y., and Bemark, M. (2010). T cell-independent IgA class switch recombination is restricted to the GALT and occurs prior to manifest germinal center formation. J. Immunol. *184*, 3545–3553.

Bouskra, D., Brézillon, C., Bérard, M., Werts, C., Varona, R., Boneca, I.G., and Eberl, G. (2008). Lymphoid tissue genesis induced by commensals through NOD1 regulates intestinal homeostasis. Nature *456*, 507–510.

Cebula, A., Seweryn, M., Rempala, G.A., Pabla, S.S., McIndoe, R.A., Denning, T.L., Bry, L., Kraj, P., Kisielow, P., and Ignatowicz, L. (2013). Thymus-derived regulatory T cells contribute to tolerance to commensal microbiota. Nature *497*, 258–262.

Chase, D.G., and Erlandsen, S.L. (1976). Evidence for a complex life cycle and endospore formation in the attached, filamentous, segmented bacterium from murine ileum. J. Bacteriol. *127*, 572–583.

Chung, H., Pamp, S.J., Hill, J.A., Surana, N.K., Edelman, S.M., Troy, E.B., Reading, N.C., Villablanca, E.J., Wang, S., Mora, J.R., et al. (2012). Gut immune maturation depends on colonization with a host-specific microbiota. Cell *149*, 1578–1593.

Craig, S.W., and Cebra, J.J. (1971). Peyer's patches: an enriched source of precursors for IgA-producing immunocytes in the rabbit. J. Exp. Med. *134*, 188–200.

Delbos, F., De Smet, A., Faili, A., Aoufouchi, S., Weill, J.C., and Reynaud, C.A. (2005). Contribution of DNA polymerase eta to immunoglobulin gene hypermutation in the mouse. J. Exp. Med. *201*, 1191–1196.

Dogan, I., Bertocci, B., Vilmont, V., Delbos, F., Mégret, J., Storck, S., Reynaud, C.A., and Weill, J.C. (2009). Multiple layers of B cell memory with different effector functions. Nat. Immunol. *10*, 1292–1299.

Fagarasan, S., Kinoshita, K., Muramatsu, M., Ikuta, K., and Honjo, T. (2001). In situ class switching and differentiation to IgA-producing cells in the gut lamina propria. Nature *413*, 639–643.

Gaboriau-Routhiau, V., Rakotobe, S., Lécuyer, E., Mulder, I., Lan, A., Bridonneau, C., Rochet, V., Pisi, A., De Paepe, M., Brandi, G., et al. (2009). The key role of segmented filamentous bacteria in the coordinated maturation of gut helper T cell responses. Immunity *31*, 677–689.

He, B., Xu, W., Santini, P.A., Polydorides, A.D., Chiu, A., Estrella, J., Shan, M., Chadburn, A., Villanacci, V., Plebani, A., et al. (2007). Intestinal bacteria trigger T cell-independent immunoglobulin A(2) class switching by inducing epithelial-cell secretion of the cytokine APRIL. Immunity *26*, 812–826.

He, B., Santamaria, R., Xu, W., Cols, M., Chen, K., Puga, I., Shan, M., Xiong, H., Bussel, J.B., Chiu, A., et al. (2010). The transmembrane activator TACI triggers immunoglobulin class switching by activating B cells through the adaptor MyD88. Nat. Immunol. *11*, 836–845.

Hooper, L.V., Littman, D.R., and Macpherson, A.J. (2012). Interactions between the microbiota and the immune system. Science *336*, 1268–1273.

Ivanov, I.I., Atarashi, K., Manel, N., Brodie, E.L., Shima, T., Karaoz, U., Wei, D., Goldfarb, K.C., Santee, C.A., Lynch, S.V., et al. (2009). Induction of intestinal Th17 cells by segmented filamentous bacteria. Cell *139*, 485–498.

Knoop, K.A., and Newberry, R.D. (2012). Isolated Lymphoid Follicles are Dynamic Reservoirs for the Induction of Intestinal IgA. Front Immunol *3*, 84.

Lathrop, S.K., Bloom, S.M., Rao, S.M., Nutsch, K., Lio, C.W., Santacruz, N., Peterson, D.A., Stappenbeck, T.S., and Hsieh, C.S. (2011). Peripheral education of the immune system by colonic commensal microbiota. Nature *478*, 250–254.

Lindner, C., Wahl, B., Föhse, L., Suerbaum, S., Macpherson, A.J., Prinz, I., and Pabst, O. (2012). Age, microbiota, and T cells shape diverse individual IgA repertoires in the intestine. J. Exp. Med. *209*, 365–377.

Lochner, M., Bérard, M., Sawa, S., Hauer, S., Gaboriau-Routhiau, V., Fernandez, T.D., Snel, J., Bousso, P., Cerf-Bensussan, N., and Eberl, G. (2011a). Restricted microbiota and absence of cognate TCR antigen leads to an unbalanced generation of Th17 cells. J. Immunol. *186*, 1531–1537.

Lochner, M., Ohnmacht, C., Presley, L., Bruhns, P., Si-Tahar, M., Sawa, S., and Eberl, G. (2011b). Microbiota-induced tertiary lymphoid tissues aggravate inflammatory disease in the absence of RORgamma t and LTi cells. J. Exp. Med. *208*, 125–134.

Macpherson, A.J., and Uhr, T. (2004). Induction of protective IgA by intestinal dendritic cells carrying commensal bacteria. Science *303*, 1662–1665.

Macpherson, A.J., Gatto, D., Sainsbury, E., Harriman, G.R., Hengartner, H., and Zinkernagel, R.M. (2000). A primitive T cell-independent mechanism of intestinal mucosal IgA responses to commensal bacteria. Science *288*, 2222–2226.

Rennert, P.D., Browning, J.L., Mebius, R., Mackay, F., and Hochman, P.S. (1996). Surface lymphotoxin alpha/beta complex is required for the development of peripheral lymphoid organs. J. Exp. Med. *184*, 1999–2006.

Shroff, K.E., Meslin, K., and Cebra, J.J. (1995). Commensal enteric bacteria engender a self-limiting humoral mucosal immune response while permanently colonizing the gut. Infect. Immun. *63*, 3904–3913.

Slack, E., Hapfelmeier, S., Stecher, B., Velykoredko, Y., Stoel, M., Lawson, M.A., Geuking, M.B., Beutler, B., Tedder, T.F., Hardt, W.D., et al. (2009). Innate and adaptive immunity cooperate flexibly to maintain host-microbiota mutualism. Science *325*, 617–620.

Slack, E., Balmer, M.L., Fritz, J.H., and Hapfelmeier, S. (2012). Functional flexibility of intestinal IgA - broadening the fine line. Front Immunol *3*, 100.

Suzuki, K., Meek, B., Doi, Y., Muramatsu, M., Chiba, T., Honjo, T., and Fagarasan, S. (2004). Aberrant expansion of segmented filamentous bacteria in IgA-deficient gut. Proc. Natl. Acad. Sci. USA *101*, 1981–1986.

Talham, G.L., Jiang, H.Q., Bos, N.A., and Cebra, J.J. (1999). Segmented filamentous bacteria are potent stimuli of a physiologically normal state of the murine gut mucosal immune system. Infect. Immun. *67*, 1992–2000.

Tannock, G.W., Miller, J.R., and Savage, D.C. (1984). Host specificity of filamentous, segmented microorganisms adherent to the small bowel epithelium in mice and rats. Appl. Environ. Microbiol. *47*, 441–442.

Tsuji, M., Suzuki, K., Kitamura, H., Maruya, M., Kinoshita, K., Ivanov, I.I., Itoh, K., Littman, D.R., and Fagarasan, S. (2008). Requirement for lymphoid tissue-inducer cells in isolated follicle formation and T cell-independent immunoglobulin A generation in the gut. Immunity *29*, 261–271.

van de Pavert, S.A., and Mebius, R.E. (2010). New insights into the development of lymphoid tissues. Nat. Rev. Immunol. *10*, 664–674.

van der Waaij, L.A., Limburg, P.C., Mesander, G., and van der Waaij, D. (1996). In vivo IgA coating of anaerobic bacteria in human faeces. Gut *38*, 348–354.

Yamamoto, M., Rennert, P., McGhee, J.R., Kweon, M.N., Yamamoto, S., Dohi, T., Otake, S., Bluethmann, H., Fujihashi, K., and Kiyono, H. (2000). Alternate mucosal immune system: organized Peyer's patches are not required for IgA responses in the gastrointestinal tract. J. Immunol. *164*, 5184–5191.